Youcef BENCHAA[1], Merabet Boulouiha Houari[1] , Denai Mouloud [2]

LAAS-National Polytechnic school-Maurice Audin *ENP ORAN, Algeria* (1), University of Hertfordshire (U.K.) (2)

doi:10.15199/48.2023.08.43

An advanced layered converter with fuzzy logic management for PV arrays

Abstract. *Due to its potential in the industrial sector, photovoltaic energy transmission has posed a fascinating challenge in recent decades. The utilisation of line transformers, which have a variety of problems including substantial voltage dips, expensive installation costs, and higher load losses, is one of the most urgent difficulties with such a system. This paper provides an alternate method based on a high-gain DC/DC interleaved boost converter with a low input voltage, a high input current, and an output voltage that is more than three times that of the typical boost converter. The input current is split over the three phases of the interleaved converter; as a result, the current stress on the circuit and the semiconductor devices is decreased, which adds to a decrease in total losses. In addition, the voltage stress is minimised compared to the interleaved converter's high output voltage. Additionally, a Maximum Power Point Tracking (MPPT) controller based on fuzzy logic control (FLC) is intended to guarantee that the PV system performs at peak efficiency. Lastly, simulation studies using the MATLAB Simulink environment are shown to demonstrate the efficacy of the suggested architecture.*

Streszczenie. *Ze względu na swój potencjał w sektorze przemysłowym fotowoltaiczna transmisja energii stanowiła fascynujące wyzwanie w ostatnich dziesięcioleciach. Wykorzystanie transformatorów liniowych, z którymi wiąże się wiele problemów, w tym znaczne spadki napięcia, wysokie koszty instalacji i większe straty obciążenia, jest jedną z najpilniejszych trudności związanych z takim systemem. W tym artykule przedstawiono alternatywną metodę opartą na przetwornicy podwyższającej napięcie DC/DC z przeplotem o wysokim wzmocnieniu, przy niskim napięciu wejściowym, wysokim prądzie wejściowym i napięciu wyjściowym, które jest ponad trzykrotnie większe niż w przypadku typowej przetwornicy podwyższającej napięcie. Prąd wejściowy jest rozdzielany na trzy fazy konwertera z przeplotem; w rezultacie zmniejsza się obciążenie prądowe obwodu i urządzeń półprzewodnikowych, co przyczynia się do zmniejszenia całkowitych strat. Ponadto napięcie napięciowe jest zminimalizowane w porównaniu z wysokim napięciem wyjściowym konwertera z przeplotem. Dodatkowo kontroler śledzenia punktu mocy maksymalnej (MPPT) oparty na sterowaniu logiką rozmytą (FLC) ma zagwarantować, że system fotowoltaiczny działa z maksymalną wydajnością. Na koniec pokazano, że badania symulacyjne z wykorzystaniem środowiska MATLAB Simulink demonstrują skuteczność sugerowanej architektury (**Zaawansowany konwerter warstwowy z zarządzaniem logiką rozmytą dla paneli fotowoltaicznych**)*

Keywords: Interleaved boost converter, Hight voltage gain, PV system, Fuzzy logic MPPT controller.
Słowa kluczowe: Przeplatany konwerter doładowania, PV, sterownik MPPT z logiką rozmytą

Introduction

The International Energy Agency (EIA) reports that renewable power output has climbed by more than 6% to reach a worldwide capacity of 8,300 TWh in 2021. This is the highest year-on-year growth since 1970.

To achieve the target of net-zero emissions by 2050, this rise is projected to increase in the coming years.

Solar photovoltaic energy constitutes a significant portion of this worldwide energy and is regarded as an appropriate alternative for supplying power to distant industrial locations, agricultural regions, and residential areas.

However, the necessity for extra equipment with Conventional DC/DC boost converter, such as booster transformers, in the PV conversion chain in order to achieve the voltage level needed by electrical networks is a significant issue increase installation complexity and expense, which represents one of the most deficiency of PV systems.

The adoption of an advanced DC/DC boost converter topology with a high gain ratio is a viable approach for obtaining the needed voltage level without a boost transformer in this instance [1].

In the literature, the interleaved boost DC/DC converter (IBC) has been used. The IBC is used in [2] for PV applications to eliminate ripples in the output current. The high voltage conversion ratio of the converter is 15.83. The findings of the experiment indicate a high voltage conversion ratio of 15.83 and a low input current ripple of 20%. This converter is suggested in [3] to lessen current ripples in the same setting.

In [4], the authors suggest an IBC-based PV system to increase the input voltage from 15 V to 400 V in the converter's discontinuous mode. In [5], the analysis and design methodology of a novel IBC DC/DC power converter architecture are described. A laboratory prototype with FPGA and DSP1104 boards was used to experimentally verify the proposed IBC converter.

The findings indicate that the IBC converter reduces the output current ripples of the fuel cell and ensures the system's dependability. In reference to estimating the ripple value of the output voltage, the authors of [6] proposed a mathematical model of an interleaved cascaded DC/DC boost converter (ICBC).

Regarding the switching frequency, duty cycle, coupling coefficient, and output voltage ripple, the ICBC circuit is evaluated.

In this research, we will develop a DC photovoltaic conversion chain using an interleaved boost converter in order to achieve a high gain ratio and optimal performance in terms of current and voltage ripples.

In addition, we will present a sophisticated fuzzy logic controller to get high-quality dynamic energy despite changing climatic restrictions.

The document is structured as follows: The second section explains the topology of a DC/DC converter.

Section 3 provides the parameters of the PV generator and the architecture of the proposed FLC-MPPT controller. The fourth section demonstrates the performance and efficacy of the proposed converter architecture and control strategy via simulation results. In addition, a comparison between the FLC and conventional P&O controllers with the proposed DC/DC converter is shown. Section 5 concludes this study with a summary of its findings.

Modeling the DC/DC Interleaved Converter

Structure of the converter

The proposed converter topology in the system is a three-level interleaved boost converter with L and C stages. The main aim of this topology is to get a higher static gain than the traditional converter and less stress on the electrical components. As shown in the circuit diagram of Fig.1, the proposed topology consists of three single-phase

boost converter with a coupled inductor for the first phase and an extension capacitor stage for each other phase. An output capacitor filter is also added to the circuit [7]

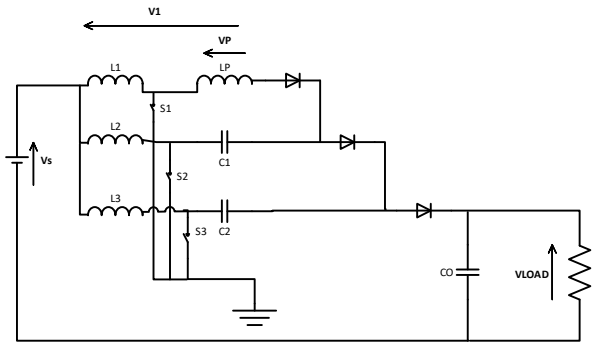

Fig.1.the proposed interleaved boost converter

Where L1,L2,L3 are phased inductors with n1 number of turns, LP is a coupled inductor with n2 number of turns, C1,C2 form the capacitor stage T, C0 represents the output filter, S1,S2,S3 denote the active switches, and D1,D2,D3 represent the rectifying diode for each phase.

.Where L1,L2,L3 are phased inductor whit n1 number off turns, LP is a coupled inductor whit n2 number off turns, C1,C2 form the capacitor stage T, C0 represents the output filter, S1,S2,S3 denote the active switches and D1,D2,D3 represent the rectifying diode for each phase.

The voltage relationship between V_P and V_1 can be given by

(1) $$N = \frac{V_1}{V_P}\ \frac{n_1+n_2}{n_1}$$

The gain ratio of the proposed converter

The gain ratio of the interleaved boost converter is given by the operating sequences the operating cycle of the DC/DC converter is composed of the following steps:

All switches activated: in this case L1, L2, L3 are charged from the supply C1, C2, LP and diodes are in off state from t0 to t1.

S1 off, S2 and S3 is activated: the inductor L2, L3 still charged from the supply; L1, discharged through the coupled inductor LP and the capacitor C1 from t1 to t2.

The third step is the same as to the first step from t3 to t4.

S2 off, S1 and S3 are activated: the inductor L1, L3 charged from the supply; L2 and C1, discharged through the coupled inductor C2, t4 to t5.

The step number five is the same as the first steps from t5 to t6.

S3 off, S1 and S2 are activated: the inductor L1, L2 charged from the supply; L3 and C2 discharged through the coupled inductor C2 through the load.

It's clear from this analyse that the voltage across the load in this dc converter is hight much more Thant the traditional converter

Voltage gain ratio expression of the converter

By using the voltage across L_1, L_2, L_3 in each state we get:

(2) $$Vs(t_1-t_0)+(V_S-V_{C1}-V_P)(t_1-t_2)+V_S(t_3-t_2)+V_S(t_4-t_3)+V_S(t_5-t_4)+V_S(t_6-t_5)=0$$

From (1) and (2) we get (3)

$$Vs(t_1-t_0)+(V_S-V_{C1})\frac{n_1}{n_1+n_2}(t_1-t_2)+V_S(t_3-t_2)+V_S(t_4-t_3)+V_S(t_5-t_4)+V_S(t_6-t_5)=0$$

And

(3) $$V_{C1}=\frac{V_S}{1-D}(1+\frac{n_2}{n_1}D)$$

For the second phase we have

(4) $$V_S(t_1-t_0)+V_S(t_1-t_2)+V_S(t_3-t_2)+(V_S-V_{C1}-V_{c2})(t_4-t_3)+V_S(t_5-t_4)+V_S(t_6-t_5)=0$$

From (3) and (4) we get

(5) $$V_{C2}=\frac{V_S}{1-D}(2+\frac{n_2}{n_1}D)$$

For the third phase we have

(6) $$V_S(t_1-t_0)+V_S(t_1-t_2)+V_S(t_3-t_2)+V_S(t_4-t_3)+V_S(t_5-t_4)+(V_S-V_{C2}-V_{CO})(t_6-t_5)=0$$

By using (5) and (6) we get the Eq (7)

(7) $$V_{C0}=\frac{V_S}{1-D}(3+\frac{n_2}{n_1}D)$$

the gain ratio off the proposed converter form Eq(7) equal to

(8) $$\boldsymbol{G=\frac{V_{load}}{VS}=\frac{V_S}{1-D}(3+\frac{n2}{n1}D)}$$

As you can see the gain ratio of the proposed converter can be written as:

$$\boldsymbol{G=\frac{V_{load}}{VS}=N\times\frac{V_S}{1-D}}$$

Where $\boldsymbol{\frac{V_S}{1-D}}$ is the duty cycle of the conventional boost converter and N>3 its means that by increasing the ratio n2/n1 it is possible to obtain an adjustable high voltage across the load and avoid using transformer which is not feasible with the conventional boost converter.

Voltage stress through the switches

the voltage stress across S1, S2 ,S3 is got it when the switch is off

(9) $$V_{stress3}=V_{load}-V_{C2}$$

$$\boldsymbol{V_{stress3}=\frac{V_S}{1-D}(3+\frac{n_2}{n_1}D)-\frac{V_S}{1-D}(2+\frac{n_2}{n_1}D)}$$

(10) $$\boldsymbol{V_{stress3}=\frac{V_S}{1-D}}$$

Similarly,

(11) $$\boldsymbol{V_{stress3}=V_{stress2}=V_{stress1}=\frac{V_S}{1-D}}$$

The voltage stress is the same as with a conventional boost, but with better performance and a higher gain voltage capability with less voltage stress. Furthermore, by increasing the number of phases, it is possible to achieve less current stress at the same duty ratio. Pulse-width modulation (PWM) is used to control the proposed DC/DC converter and limit the number of sequences. Each phase of the interleaved converter is limited and shifted by 120° from the previous phase, and all phases have the same duty cycle [8].

Sequences limits

To control the proposed DC/DC converter and limit its sequences, we used the switching pulse-width-modulated (PWM) with switching frequency FC; each phase of the interleaved converter is limited and shifted by 120° from the previous phase; all phases have the same duty cycle D. [5]

Modelling and control of the photovoltaic

Modelling of the PVG

As shown in Fig. 2, the PV cell model used is a one-diode model, which consists of a shunt resistance (high value in the order of k) accounting for the loss with a small leakage current through the parallel path, a series resistance accounting for the losses, which include metal grid, contacts, and current collecting bus losses, and a

diode representing a cross current associated with p-n junction, semiconductor devices [9],

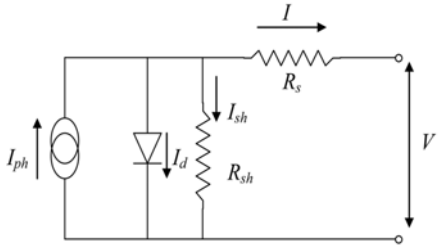

Fig.2. electrical model of PV cell

The output current of each cell is given by

(12) $$I = \left(I_{pv\,n} + K_I \Delta T\right)\frac{G}{G_n} - I_0\left(e^{\frac{(V_{pv}+R_s I}{\alpha V_T}} - 1\right) - \frac{V+R_s I}{R_{sh}}$$

Where I0 denotes the diode saturation currents and is given by:

(13) $$I_0 = \frac{I_{SC}+K_I\Delta_T}{e^{\left(\frac{V_{OC}+K_v\Delta_T}{\alpha V_T}\right)}-1}$$

(14) $$Ipv = \frac{R_{sh}+R_s}{R_{sh}} I_{sc}$$

I_{SC}= short-circuit current; V_{OC}= open-circuit voltage; V_T= thermal tension; R_s= serial resistor; R_{sh}= Shunt resistor
α= ideality factor of the junction.; K = Boltzmann constant (1.38 .10-23 J/K); G_n= solar radiation under standard conditions; G=solar radiation; V = PV voltage

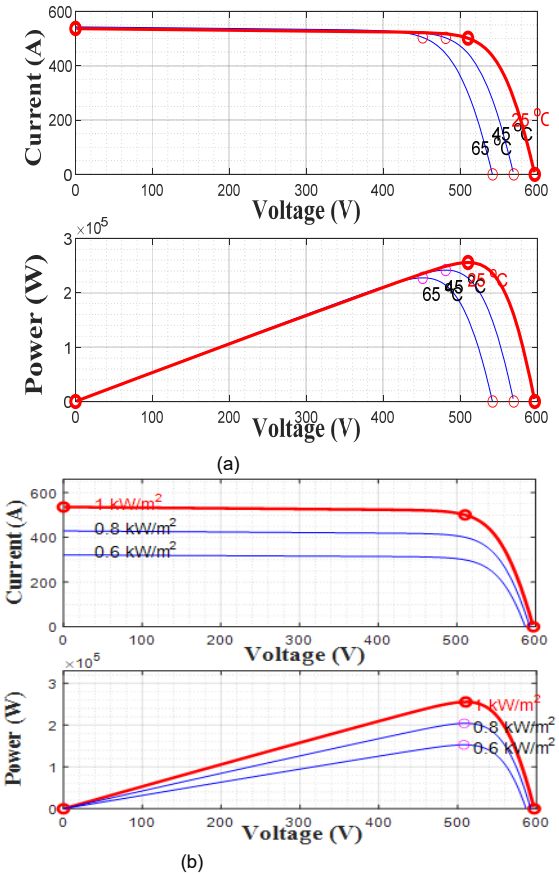

Fig.3. PVG I-V and P-V characteristics (a) temperature variation, (b) irradiance variation.

The current-voltage (I-V) and power-voltage (P-V) characteristics of the PVG for different temperature and irradiance values are plotted in Figure 3.

A temperature increase causes the open-circuit voltage to decrease without any considerable change in the short-circuit current whereas an increase in the irradiance leads to an increase in the short-circuit current while the open-circuit voltage remains unchanged. To maintain the operating point of the PV cell at the maximum power requires the implementation of an MPPT controller

MPPT control strategy based on FLC

Fuzzy logic controller design

The inputs to the FLC are the error (E) and the error change (ΔE) defined as follows [10]–[26]:

(15) $$E = \frac{P_{PV}(t)-P_{PV}(t-1)}{V_{PV}(t)-V_{PV}(t-1)}$$

(16) $$\Delta E = E(t) - E(t-1)$$

Where $P_{PV}(t)$ is power, $V_{PV}(t)$ is voltage of the PV panel and $P_{PV}(t-1), V_{PV}(t-1)$are the previous values of the power and voltage of PV panel respectively.
The operation of the MPPT-FLC is illustrated in Figure 4.

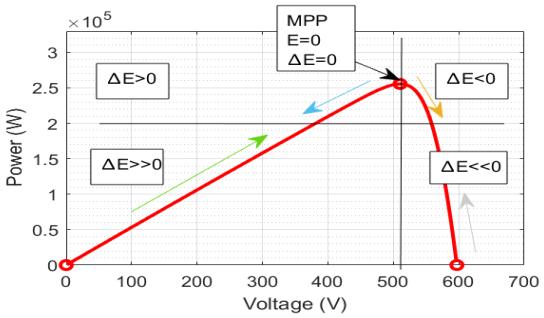

Fig.4. FLC input error value according to P-V characteristic.

(i) When $\Delta P > 0$ and $\Delta V < 0$, to reach the MPP, the voltage should be decreased (grey arrow).
(ii) When $\Delta P < 0$ and $\Delta V > 0$, to reach the MPP, the voltage should be decreased (orange arrow).
(iii) When $\Delta P < 0$ and $\Delta V < 0$, to reach the MPP, the voltage should be increased (blue arrow).
(iv) When $\Delta P > 0$ and $\Delta V > 0$, to reach the MPP, the voltage should be increased (green arrow).
By using the change in error, we can adjust the speed of response of the FLC. The output of the FLC is the control action K to adjust the duty cycle D.
The rules of the FLC are given in Table 1

Table 1: FLC rules

E / ΔE	NB	NS	Z	PS	PB
NB	ZE	ZE	NS	PS	PB
NS	ZE	ZE	ZE	PS	PB
Z	NG	NS	ZE	PS	PB
PS	NG	NS	ZE	Z	Z
PB	NG	NS	PS	Z	Z

NB=' negative Big'; NS='negative Small'; Z='Zeros'; PS='positive Small'; PB='positive Big'
The output of the fuzzy controller is obtained from the defuzzification using the centroid algorithm where the duty cycle is:

(17) $$D(t) = D(t-1) + K(t)$$

The membership functions for the inputs and output are depicted in Figure 6

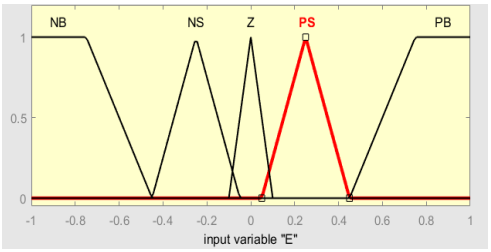

(a)

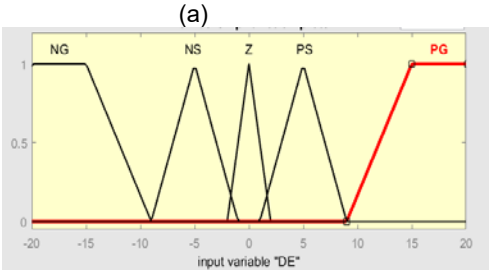

(b)

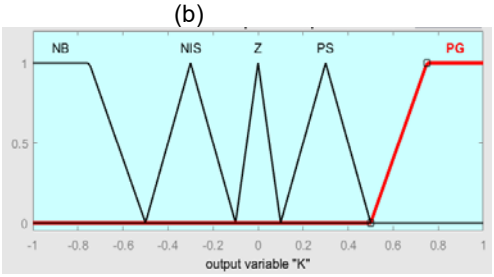

(c)

Fig.6. (a) The input of FLC (Error, E), (b) The input of FLC (Change of error, DE) (c) The output of FLC correction of duty K.

Simylation results and discussion

The PV system with the three-level interleaved DC/DC boost converter and the MPPT controller are simulated using MATLAB/Simulink. The parameters of the model are listed in (Table 2 and 3). The PV generator with a capacity of 25.5 kW consists of 616 PV module (88 Parallel x 7 in series).

Table 2. Electrical characteristic of PV panel

Electrical characteristic	Value
Open-circuit voltage (V_{oc})	85.83 V
Short-circuit current (I_{sc})	6.09 A
Optimum operating voltage (V_{mpp})	72.9 V
Optimum operating current (I_{mpp})	5.69 A
Maximum power at STC (P_{max})	414.5 W
Current temperature coefficient of I_{sc}	0.031
Voltage temperature coefficient of V_{oc}	-0.229

Table 3. Parameter of the interleaved converter [17]

Parameter	Value
$C_1 = C_2 = \frac{Vpv \times D \times TC}{\Delta V \times R} =$	0.33e-6F
$L_1 = L_2 = L_3 = \frac{Vpv \times D \times TC}{\Delta Iph}$ $FOR \ \ I_{ph} = \frac{I}{3}$	200e-4H
$L_P = N^2 \times L_1$	1800e-4H
C0	5e − 6F
S_F	33KHZ

The simulation study includes two parts: Part 1 is a comparison between the proposed converter topology and the conventional converter. Part 2 is the evaluation of the overall system (PV/ proposed converter/MPPTcontrollers) performance under temperature and irradiance variations. A comparison of the proposed MPPT-FLC and the Perturb and Observe (P&O) MPPT algorithm

Performances of the interleaved boost converter

To verify the performance of the advanced converter, we simulate the PVG under the standard condition (T = 25° and G = 1000 w/m2) connected with the conventional boost converter on the first case and with the advanced dc/dc converter on the second case with duty ratio D = 0.8 in each case. We also give n2/n1 = 3.

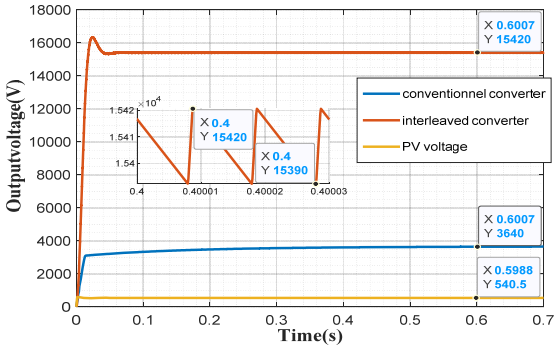

Fig.7. The output voltage waveform for DC/DC converter

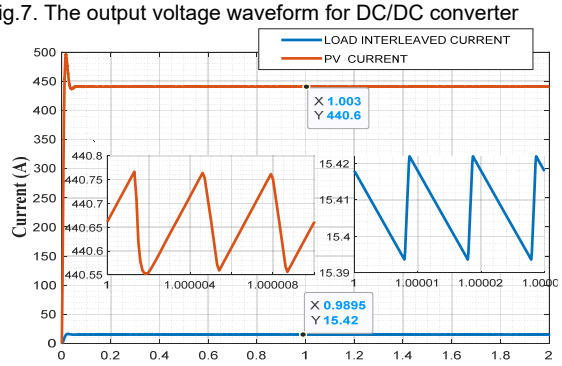

Fig.8. current and ripple for interleaved boost converter

The simulation result indicates that the suggested converter creates 15420 V from an input VPV of 540.5 V with a duty ratio of D = 0.8, which corresponds to a voltage gain of M = 28.6. In contrast, the conventional converter generates only 3640 V from the same input. This indicates that the conventional converter provides the same output as the suggested converter with a duty ratio of D = 0.97, which is extremely high and will result in a serious reverse recovery issue. Similarly, the voltage stress for the converter is 3640V. With the interleaved converter, the load current decreased to 15.42 A from 440.6 A with the conventional converter.

The output ripple voltage of the interleaved boost converter is 0.19 percent of the nominal output voltage, and the output ripple current is 0.004 percent of the output current. The switch current stress is minimized when the input current is split between three phases, resulting in less switch loss.

Fuzzy logic controller performance

In this part, the global system (PV+proposed converter) under various different condition:
Case1: T=25°and G=1000W.
Case2: T=45°and G=1000W.
Case3: T=25°and G=800W.

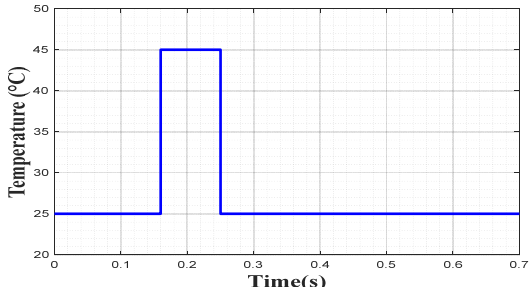

(a)

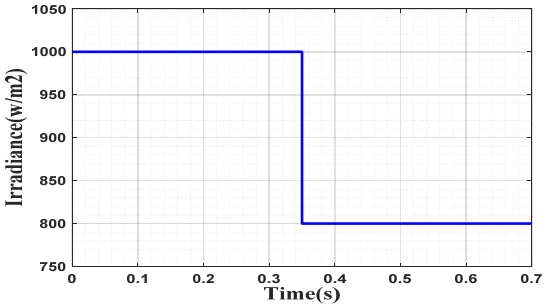

(b)

Fig. 9. (a) Temperature, (b) Solar radiation waveform

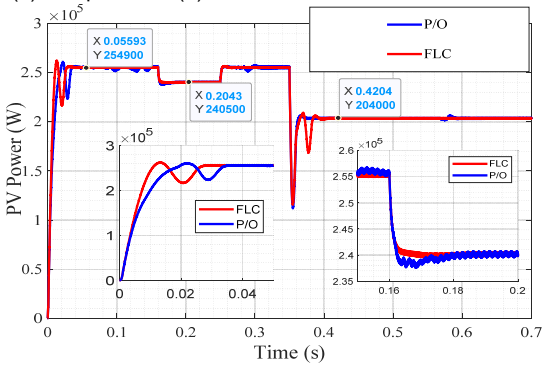

Fig. 10. PV power waveform

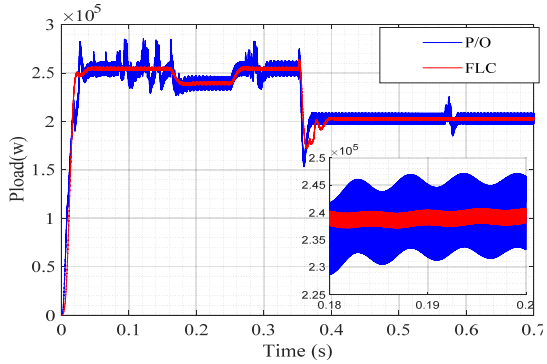

(a)

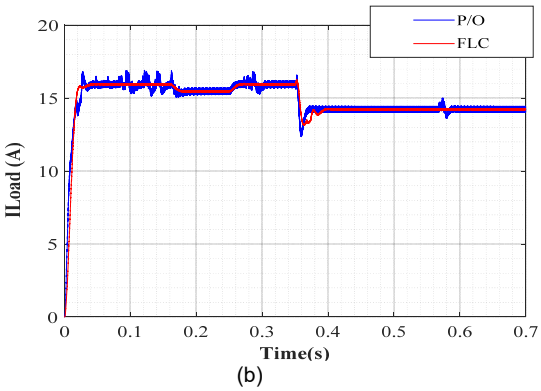

(b)

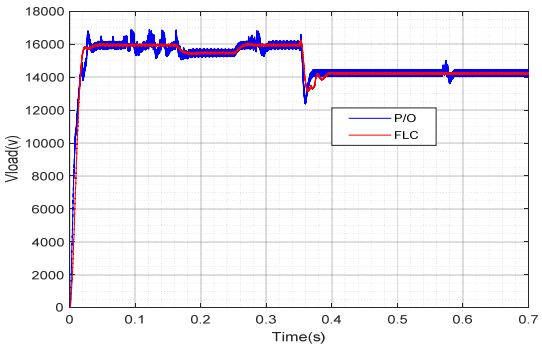

(c)

Fig.11. (a) Load power waveform, (b)Load current waveform, (c)Load voltage waveform

The FL-based MPPT controller lowered the response time to 0.0021s (case 1) in detailed figure Fig. 10 in order to attain the MPP more quickly than P&O.

The system achieved the MPP point with FL Control and PO Control in each instance. Fig 10

In order to reach the MPP, as shown in Fig. 11's detailed figure (a), the operation point of the P&O continues to oscillate due to the continual disturbance of the operating voltage. In contrast, this effect is not observed in FL-based MPPT techniques, where signals of power, voltage, current, and duty ratio are nearly constant.

Figure 11.b and 11.c depicts the effect of the typical controller's continued disturbance. On the load side, where an interleaved converter with a higher gain ratio is used, the volatility of the electrical parameters (current, voltage, and power) is significantly greater than when the FL control is used, as illustrated in each picture.

Conclusion

The proposed system has been studied and compared under different conditions, where the accuracy of the system under irradiance and temperature change varies between 99.5% and 99.8%. The use of an interleaved boost converter gives more flexibility in the output voltage variation range than is possible with a traditional boost converter. To improve the load energy quality, high-gain converters require a controller with high accuracy; the fuzzy logic controller is an ideal solution when compared to a P/O controller. The impact of this study is to achieve low-cost PV energy with the use of the advanced topologies of interleaved converters to get high dc voltage from low input PV voltage, which represents a solution to avoid the use of the boost transformer and reduce the size and weight of magnetic circuits. This topology can be used in a photovoltaic grid intended for transport.

Acknowledgments

Our special thanks to the examiners for their constructive comments. The authors are grateful to Laboratory of automation and analyse of systems, Ministry of Higher Education and Scientific Research of Algeria for its continuous assistance in scientific research

***Authors**: PhD student BENCHAA Youcef Laboratory of Automation and Anlayse of systeme LAAS-* National Polytechnic school-Maurice Audin *ENP ORAN, Algeria , E-mai:youcef.benchaa@enp-oran.dz; Pr MERABET Houari Boulhouina Ecole Normale Polytechnique, ENP ORAN, Algeria*
E mail: Houari.merabet@gmail;com
Pr Mouloud Denaï University of Hertfordshire (U.K.)

REFERENCES

[1] A. Alzahrani, “Scholars’ Mine Scholars’ Mine Doctoral Dissertations Student Theses and Dissertations Advanced topologies of high-voltage-gain DC-DC boost Advanced topologies of high-voltage-gain DC-DC boost converters for renewable energy applications converters for renewable energy applications,” 2018.

[2] B. Sri Revathi, P. Mahalingam, and F. Gonzalez-Longatt, “Interleaved high gain DC-DC converter for integrating solar PV source to DC bus,” Solar Energy, vol. 188, pp. 924–934, Aug. 2019,

[3] M. Veerachary, “Switched L-C Cell Based Interleaved Boost Converter,” in 2020 IEEE International Conference on Power Electronics, Drives and Energy Systems (PEDES), Dec. 2020, pp. 1–5.

[4] M. Altimania, A. Alzahrani, M. Ferdowsi, and P. Shamsi, “Operation and Analysis of Non-Isolated High-Voltage-Gain DC-DC Boost Converter with Voltage Multiplier in the DCM,” in 2019 IEEE Power and Energy Conference at Illinois (PECI), Feb. 2019, pp. 1–6.

[5] S. Farhani, A. N’Diaye, A. Djerdir, and F. Bacha, “Design and practical study of three phase interleaved boost converter for fuel cell electric vehicle,” J Power Sources, vol. 479, p. 228815, Dec. 2020

[6] K. Sabanci and S. Balci, “Development of an expression for the output voltage ripple of the DC-DC boost converter circuits by using particle swarm optimization algorithm,” Measurement, vol. 158, p. 107694, Jul. 2020,

[7] “A Three Phase Interleaved Boost Converter with L & C Voltage Extension Mechanism,” Tehnicki vjesnik - Technical Gazette, vol. 25, no. 1, Feb. 2018

[8] M. A. Harimon, A. Ponniran, A. N. Kasiran, and H. H. Hamzah, “A Study on 3-phase Interleaved DC-DC Boost Converter Structure and Operation for Input Current Stress Reduction,” International Journal of Power Electronics and Drive System (IJPEDS), vol. 8, no. 4, pp. 1948–1953, 2017,

[9] S. Motahhir, A. el Ghzizal, and A. Derouich, “Modélisation et commande d’un panneau photovoltaïque dans l’environnement PSIM.

[10] Y. Chaibi, A. Allouhi, M. Malvoni, M. Salhi, and R. Saadani, “Solar irradiance and temperature influence on the photovoltaic cell equivalent-circuit models,” Solar Energy, vol. 188, pp. 1102–1110, Aug. 2019,

[11] U. Yilmaz, A. Kircay, and S. Borekci, “PV system fuzzy logic MPPT method and PI control as a charge controller,” Renewable and Sustainable Energy Reviews, vol. 81. Elsevier Ltd, pp. 994–1001, Jan. 01, 2018.

[12] A. Ali et al., “Investigation of MPPT Techniques Under Uniform and Non-Uniform Solar Irradiation Condition–A Retrospection,” IEEE Access, vol. 8, pp. 127368–127392, 2020,

[13] B. Bendib, H. Belmili, and F. Krim, “A survey of the most used MPPT methods: Conventional and advanced algorithms applied for photovoltaic systems,” Renewable and Sustainable Energy Reviews, vol. 45, pp. 637–648, May 2015,

[14] J. Kumar, B. Rathor, and P. Bahrani, “Fuzzy and P&O MPPT Techniques for Stabilized the Efficiency of Solar PV System,” in 2018 International Conference on Computing, Power and Communication Technologies (GUCON), Sep. 2018, pp. 259–264.

[15] K. Yung Yap, C. R. Sarimuthu, and J. Mun-Yee Lim, “Artificial Intelligence Based MPPT Techniques for Solar Power System: A review,” Journal of Modern Power Systems and Clean Energy, vol. 8, no. 6, pp. 1043–1059, 2020,

[16] S. Samal, P. K. Barik, and S. K. Sahu, “Extraction of maximum power from a solar PV system using fuzzy controller based MPPT technique,” in 2018 Technologies for Smart-City Energy Security and Power (ICSESP), Mar. 2018, pp. 1–6.

[17] S. Sumathi, L. Ashok Kumar, and P. Surekha, “Green Energy and Technology

[18] I. Yadav, S. K. Maurya, and G. K. Gupta, “A literature review on industrially accepted MPPT techniques for solar PV system,” International Journal of Electrical and Computer Engineering, vol. 10, no. 2. Institute of Advanced Engineering and Science, pp. 2117–2127, 2020.

[19] A. S. Samosir, H. Gusmedi, S. Purwiyanti, and E. Komalasari, “Modeling and Simulation of Fuzzy Logic based Maximum Power Point Tracking (MPPT) for PV Application,” International Journal of Electrical and Computer Engineering (IJECE), vol. 8, no. 3, p. 1315, Jun. 2018,

[20] M. A. Abo-Sennah, M. A. El-Dabah, and A. E.-B. Mansour, “Maximum power point tracking techniques for photovoltaic systems: a comparative study,” International Journal of Electrical and Computer Engineering (IJECE), vol. 11, no. 1, p. 57, Feb. 2021

[21] J. Kumar, B. Rathor, and P. Bahrani, “Fuzzy and P&O MPPT Techniques for Stabilized the Efficiency of Solar PV System,” in 2018 International Conference on Computing, Power and Communication Technologies (GUCON), Sep. 2018, pp. 259–264.

[22] A. Chaithanakulwat, “Track the maximum power of a photovoltaic to control a cascade five-level inverter a single-phase grid-connected with a fuzzy logic control,” International Journal of Power Electronics and Drive Systems (IJPEDS), vol. 10, no. 4, p. 1863, Dec. 2019

[23] A. A. AlZubaidi, L. Abdul Khaliq, H. Salman Hamad, W. Khalid Al-Azzawi, M. Sameer Jabbar, and T. Abdulwahhab Shihab, “MPPT implementation and simulation using developed P&O algorithm for photovoltaic system concerning efficiency,” Bulletin of Electrical Engineering and Informatics, vol. 11, no. 5, pp. 2460–2470, Oct. 2022,

[24] K. W. Nasser, S. J. Yaqoob, and Z. A. Hassoun, “Improved dynamic performance of photovoltaic panel using fuzzy Logic-MPPT algorithm,” Indonesian Journal of Electrical Engineering and Computer Science, vol. 21, no. 2, p. 617, Feb. 2021,

[25] V. Subramanian, V. Indragandhi, R. Kuppusamy, and Y. Teekaraman, “Modeling and analysis of pv system with fuzzy logic mppt technique for a dc microgrid under variable atmospheric conditions,” Electronics (Switzerland), vol. 10, no. 20, Oct. 2021,

[26] SURYOATMOJO, H., Ashari, M., & ARUMSARI, N. Design and Implementation of MPPT Fuzzy Logic Controller for Inverter Connected to Water Pump.